Thermochimica Acta 509 (2010) 120–127

Contents lists available at ScienceDirect

Thermochimica Acta

journal homepage: www.elsevier.com/locate/tca

Synthesis, structure, thermal and luminescent behaviors of lanthanide—Pyridine-3,5-dicarboxylate frameworks series

Renata Łyszczek*

Department of General and Coordination Chemistry, Faculty of Chemistry, University of Maria Curie-Skłodowska, M.C. Skłodowskiej Sq. 2, 20-031 Lublin, Poland

ARTICLE INFO

Article history:
Received 25 March 2010
Received in revised form 10 June 2010
Accepted 12 June 2010
Available online 18 June 2010

Keywords:
MOFs
Lanthanides
TG-DSC
TG-FTIR
Luminescence

ABSTRACT

The isostructural series of lanthanide pyridine-3,5-dicarboxylates of the formula $[Ln_2pdc_3(dmf)_2]\cdot(dmf)_x(H_2O)_y$ where Ln are lanthanides from La(III) to Lu(III); pdc^{2-} – $C_5H_3N(COO)_2$; dmf – N,N′-dimethylformamide have been prepared under solvothermal conditions. The X-ray analyses show that the complexes are three-dimensional frameworks possessing one-dimensional rhomboid channels occupied by disordered solvent molecules. Thermal behavior of the complexes has been investigated using the TG/DSC and TG/FTIR measurements. The luminescence properties of the Eu(III) and Tb(III) complexes have been studied. They show very strong characteristic emissions in the red and green regions, respectively.

1. Introduction

Metal–organic frameworks (MOFs) have attracted huge attention as a new class of hybrid porous solids. Large surface area, low density and controllable channel size as well as acceptable thermal stability make them promising materials in a wide variety of fields like: gas storage (hydrogen, carbon dioxide, methane, hydrogen, oxygen) and gas separation (notably greenhouse gases), organic synthesis, and heterogeneous catalysis [1–13]. Metal–organic frameworks are well characterized by crystalline architectures, which can be self-assembled by the coordination of metal ions with bridging linkers (O or/and N donors). Construction of such compounds is governed not only by the coordination geometry of the metal ions but also by their affinity for donor atoms. As reported in the literature, the majority of the investigated metal–organic frameworks are based on the first raw of d-block transition metal centers [14–20], whereas the lanthanide coordination polymers are less documented. Variable and high coordination numbers as well as a wide variety of coordination environments of lanthanide cations may cause difficulty in the design and synthesis of lanthanide coordination polymers of desirable topology. On the other hand, coordination polymers containing lanthanide ions form fascinating structures along with the special magnetic and luminescence properties [21–25], that make them useful in material science including light conversion molecular devices i.e. light sources, detector systems, light-emitting diodes, solid state lasers [26–29]. The lanthanide ions are characterized by unique optical properties due to their spectrally narrow f-f electronic transitions. Unfortunately, lanthanide transitions are forbidden by Laporte selection rules that cause to weak absorbance and low quantum yields [28,30]. Complexation of the Ln(III) ions with strongly absorbing ligands leads to the formation of luminescent MOF devices by the energy transfer from the linker excited state to the appropriate metal level. This coupling leads to the increase in luminescence and is widely known as the “antenna” effect.

Since, the lanthanide ions have high affinity for ligands containing oxygen atoms, policarboxylate linkers such as terephthalic [31–34], trimesic [35–38] and 2,6-naphthalenedicarboxylic [39–41] acids are widely used in the synthesis of lanthanide–organic frameworks. On the other hand, pyridine-3,5-dicarboxylic acid is exploited in the synthesis of coordination polymers due to its rigid multidentate character as well as “antenne” character [42,43].

As was mentioned above, metal–organic frameworks are widely explored due to their potential applications. One of the most important requirements imposed to the MOFs apart from rigid and porous structure is their thermal stability under air conditions [41]. Usage of the coordination polymers of transition metals at high temperature is limited due to their weak thermal stability (up to about 300 °C) [15,17]. On the contrary lanthanide complexes form more thermally stable compounds that provide opportunities for their applications at higher temperature [24,39,37].

The methods of thermal analysis not only allow to determine the thermal stability of the coordination polymers but

* Tel.: +48 81 537 57 43.
E-mail address: renata.lyszczek@poczta.umcs.lublin.pl.

0040-6031/$ – see front matter © 2010 Elsevier B.V. All rights reserved.
doi:10.1016/j.tca.2010.06.010

are also indispensable tools for the estimation of solvent contents in channels. The characteristic structural feature of the microporous metal–organic frameworks is formation of three-dimensional skeletons with the channels occupied by solvent molecules. They are highly disordered and it is impossible to locate them by the X-ray diffraction measurements. The next very important application of thermal analysis (especially coupled techniques TG-FTIR) in investigations of microporous coordination polymers is recognization of type of solvent molecules distributed within the channels. The syntheses of MOFs are very often carried out by the solvothermal method using a mixture of solvents. Due to different affinity of solvent molecules for the metal–organic framework, different molecules can be included into the pores. For such a reason, a number of papers dealing with thermal characteristics of coordination polymers still increases [44–46]. There were applied thermal analysis methods also in course of kinetic investigations of desolvation process in coordination polymers as well as determination of thermodynamic function of these compounds [47–51].

So far, no systematic investigations across the lanthanide pyridine-3,5-dicarboxylate series obtained by the solvothermal method have been carried out. Hitherto, investigations on pyridine 3,5-dicarboxylates only with selected lanthanide ions such as erbium(III), ytterbium(III) [52] and europium(III) [53] obtained by means of solvothermal method have been described.

Following my ongoing research attempts toward the synthesis of lanthanide polycarboxylates coordination polymers [54–56], in my previous work, I investigated the complexes of light lanthanides (from La to Gd) with dinicotinic acid obtained by the classical method [57]. Herein, I have reported a series of lanthanide(III) complexes with pyridine-3,5-dicarboxylic acid obtained by the solvothermal method from N,N′-dimethylformamide solution.

The intention of the presented paper was to determine the thermal properties of the investigated lanthanide dinicotinates by TG-DSC and TG-FTIR methods in correlation with their crystal structures. The results from the thermogravimetric and differential thermal calorimetry allowed to obtain information concerning with thermal decomposition of complexes in air and argon atmosphere. The TG-FTIR method was applied as an excellent technique for qualitative determination of molecules included in the channels which was impossible from the X-ray single-crystal analysis. The next scope of this paper was to found out, the differences among series of isostructural lanthanide dinicotinates based on thermal investigations. Additionally, the luminescence properties of Eu(III) and Tb(III) complexes have been investigated.

2. Experimental

The studied compounds were prepared by reacting of 1.5mmol of pyridine-3,5-dicarboxylic acid (dinicotinic acid) (250 mg) with lanthanide(III) chloride hydrates (obtained by dissolving of 0.5mmol of lanthanide oxide in hydrochloric acid) in 10 mL N,N′-dimethylformamide by a solvothermal technique, in Teflon-lined autoclaves which were heated under an autogenous pressure to 140 °C for 5 days and then cooled to room temperature for 24 h.

The infrared spectra of the complexes and pyridine-3,5-dicarboxylic acid were recorded in KBr discs on a SPECORD M80 spectrophotometer over the range 4000–400 cm^{-1}. The X-ray powder diffractions of the studied complexes were recorded on a HZG 4 diffractometer, using Ni filtered CuK_α radiations. Measurements were taken over the range of $2\theta = 5–70°$.

Thermal analyses of the prepared complexes were carried out by the TG-DSC method using the SETSYS 16/18 analyser (Setaram). The samples (about 5–9 mg) were heated in ceramic crucibles up to 850 °C at a heating rate of 10 °C min^{-1} in dynamic air atmosphere ($v = 0.75\ dm^3\ h^{-1}$).

The TG-FTIR coupled measurements have been carried out using a Netzsch TG apparatus coupled with a Bruker FTIR IFS66 spectrophotometer. The samples of about 7–12 mg were heated up to 1000 °C at a heating rate of 10 °C min^{-1} in flowing argon atmosphere.

The luminescence spectra were recorded in the solid state at room temperature on the FP-6300 Jasco fluorescence spectrometer.

Single-crystal diffraction data were measured at room temperature in the $\omega/2\theta$ mode on the Oxford Diffraction Xcalibur diffractometer using the graphite-monochromated Mo K_α radiation ($\lambda = 0.71073$ Å). Crystal structures were solved by direct methods using SHELXS97 [58] and refined by the full-matrix least-squares on F^2 using the SHELXL97 program [59].

3. Results and discussion

The reaction of lanthanide(III) salts with pyridine-3,5-dicarboxylic acid in the N,N′-dimethylformamide solution leads to the formation of complexes of the general formula: $[Ln_2pdc_3(dmf)_2]\cdot(dmf)_x(H_2O)_y$, where Ln = lanthanides from La(III) to Lu(III); pdc – $C_5H_3N(COO)_2{}^{2-}$, dmf – N,N′-dimethylformamide molecules, $x = 0.5–1$, $y = 1$ or 0. The detailed formulas of complexes as well as their elemental analyses are given in Table 1.

The obtained complexes are hardly soluble in water as well as in the common organic solvents such as methanol, ethanol, N,N′-dimethylformamide, tetrahydrofuran, dimethyl sulfoxide and benzene.

3.1. Structural description

Under solvothermal conditions, the investigated compounds have been grown in the in the form of like-needle transparent crystals. Unfortunately, they were not suitable for complete X-ray single-crystal measurements because of their fragility. For some monocrystals, it was possible to determine the framework of the crystal structure whereas large disorder of solvent molecules included in the channels caused incapability of precise determination of uncoordinated solvent molecules. These molecules were determined by thermogravimetric and elemental measurements. The unit cell parameters from the selected compounds given in Table 2 reveal that the complexes are isostructural, which is further confirmed by the powder X-ray diffraction method (Fig. 1) and IR measurements. The lanthanide dinicotinates crystallize in the orthorhombic system and Pnma space group. The parameters of cell units are very similar and the only differences observed are a result of lanthanide contraction. The whole series of the investigated compounds is isotructural with pyridine-3,5-dicarboxylates of Eu [53], Er and Y [52] previously reported.

The complexes obtained from dmf solution form three-dimensional polymeric structures while compounds synthesized under hydrothermal conditions constitute the 1D two stranded polymeric chains [42]. The frameworks of reported complexes are built up from pyridine-3,5-dicarboxylate linkers and Ln(III) ions. Each Ln(III) is coordinated by eight oxygen atoms derived from six pyridine-3,5-dicarboxylate molecules. Carboxylate groups are of threedentate bridging-chelating and bidentate bridging character. Additionally, the central atom is coordinated by the carbonyl oxygen atom of the monodentate dmf molecule. The structures possess 1D channels occupied by totally disordered N,N′-dimethylformamide and water molecules in the crystal lattice. As the affinity of oxygen atoms for lanthanide atoms is greater than for nitrogen atoms, coordination of the dinicotinate ligand by N atom does not take place. In the coordination polymers of transition metals with dinicotinate liagnds, nitrogen atoms always participate in metal bonding [60–62].

Table 1
Results of elemental analyses of lanthanide complexes with dinicotinic acid and dmf.

Complex	%C		%H		%N	
	Calc.	Found	Calc.	Found	Calc.	Found
$[La_2pdc_3(dmf)_2]\cdot dmf_{0.5}(H_2O)$	35.13	34.82	2.93	2.75	7.86	7.56
$[Ce_2pdc_3(dmf)_2]\cdot dmf_{0.5}(H_2O)$	35.04	39.21	2.92	2.65	7.88	7.63
$[Pr_2pdc_3(dmf)_2]\cdot dmf_{0.5}(H_2O)$	35.16	34.79	2.93	2.76	7.92	7.51
$[Nd_2pdc_3(dmf)_2]\cdot dmf_{0.5}(H_2O)$	36.29	35.65	3.02	2.85	8.17	8.10
$[Sm_2pdc_3(dmf)_2]\cdot dmf(H_2O)$	34.84	34.62	3.29	3.02	8.13	7.87
$[Eu_2pdc_3(dmf)_2]\cdot dmf_{0.5}(H_2O)$	35.74	35.61	2.98	2.76	8.05	7.78
$[Gd_2pdc_3(dmf)_2]\cdot\ dmf_{0.5}(H_2O)$	33.84	33.56	2.82	2.56	7.62	7.54
$[Tb_2pdc_3(dmf)_2]\cdot dmf$	34.88	34.76	3.10	2.87	8.14	7.38
$[Dy_2pdc_3(dmf)_2]\cdot dmf$	34.64	34.42	3.08	2.76	8.08	7.86
$[Ho_2pdc_3(dmf)_2]\cdot dmf$	34.48	34.01	3.06	2.81	8.04	7.71
$[Er_2pdc_3(dmf)_2]\cdot dmf$	34.33	33.89	3.05	2.86	8.01	7.92
$[Tm_2pdc_3(dmf)_2]\cdot dmf$	34.22	33.67	3.04	2.76	7.98	7.66
$[Yb_2pdc_3(dmf)_2]\cdot dmf$	33.99	33.52	3.02	2.84	7.93	7.63
$[Lu_2pdc_3(dmf)_2]\cdot dmf$	34.22	33.67	3.04	2.68	7.98	7.53

Table 2
The unit cell parameters of lanthanide complexes with pyridine-3,5-dicarboxylic acid and dmf.

	Orthorhombic system, Pnma space group			
	a (Å)	b (Å)	c (Å)	Z (Å^3)
$[La_2pdc_3(dmf)_2]\cdot dmf_{0.5}(H_2O)$	8.224(2)	30.284(6)	15.71893)	3914.7(4)
$[Ce_2pdc_3(dmf)_2]\cdot dmf_{0.5}(H_2O)$	8.201(4)	30.190(5)	15.686(6)	3883(4)
$[Tb_2pdc_3(dmf)_2]\cdot dmf$	8.557(1)	28.511(7)	15.939(1)	3888.58
$[Ho_2pdc_3(dmf)_2]\cdot dmf$	8.517(1)	28.458(4)	15.806(1)	3830.92
$[Yb_2pdc_3(dmf)_2]\cdot dmf$	8.438(1)	28.43(4)	15.693(1)	3762(9)

The spectra of free acid as well as the described complexes were recorded in the infrared range (Fig. 2). All complexes show a broad absorbance band in the range 3400–3200 cm^{-1} characteristic of the stretching vibrations of OH bonds from water molecules as well as hydrogen bonds. The bands at 3060 and 2924 cm^{-1} were ascribed to the stretching vibrations of the CH bonds in the CH_3 groups of N,N′-dimethylformamide molecules. The bands derived from stretching the C=O group from dmf appear in the range 1690–1650 cm^{-1}. The strong band at 1656 cm^{-1} can be assigned to the coordinated carbonyl groups whereas the remaining weak bands are derived from physically bonded dmf molecules [63]. Deprotonation of pyridine-3,5-dicarboxylic acid was confirmed by the absence of the stretching vibrations of C=O at 1720 cm^{-1} [64].

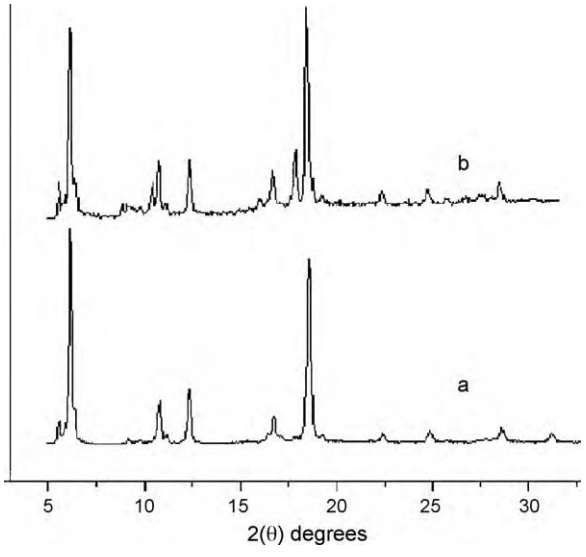

Fig. 1. XRD patterns of (a) $[Nd_2pdc_3(dmf)_2]\cdot dmf_{0.5}(H_2O)$ and (b) $[Tm_2pdc_3(dmf)_2]\cdot dmf$.

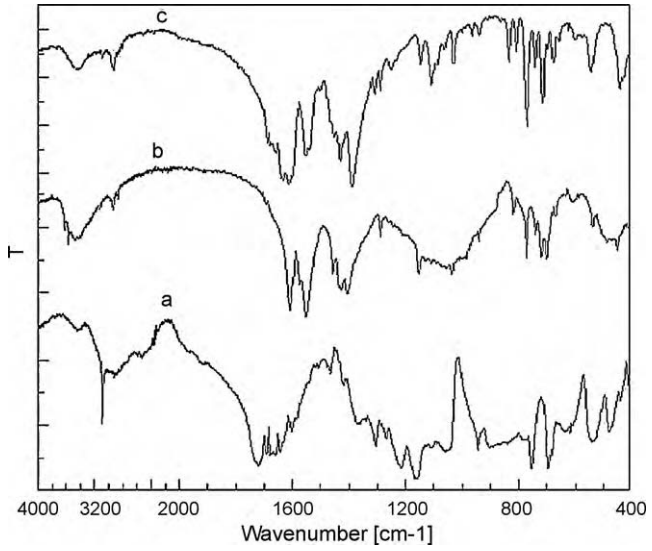

Fig. 2. IR spectra of (a) pyridine-3,5-dicarboxylic acid; (b) $[Nd_2pdc_3(dmf)_2]\cdot dmf_{0.5}(H_2O)$ and (c) $[Er_2pdc_3(dmf)_2]\cdot dmf$.

Thus the spectra of the lanthanide complexes show the bands originating from carboxylate groups bands in the range 1600–1560 and 1400–1380 cm^{-1} from the stretching asymmetric and symmetric vibrations, respectively [65–66]. These data are in good agreement with the crystal structures determined by X-ray analysis.

The bands from the stretching asymmetric vibrations are split that is typical of unequivalency of carboxylate groups. The infrared spectra confirm that carboxylate groups are of three-dentate bridging-chelating and bidentate-bridging character. The strong band at 1552 cm^{-1} was assigned to the coupled vibration of deformation and rocking vibration of CH_3 group as well as stretching vibrations of CN bond from the dmf molecules.

3.2. Thermal analysis

To study thermal decomposition of these complexes, the thermogravimetric analysis (TG) and the differential scanning calorimetry (DSC) were performed for crystalline samples. The investigated complexes decompose in the identical way during heating in the temperature range 30–400 °C in air as well as in argon atmosphere (Figs. 3 and 4). In such temperature, only solvent molecules are evolved, and changing of atmosphere does not influence on the way of desolvatation. Obviously, slight differences in the temperature of processes can be observed due to presence of

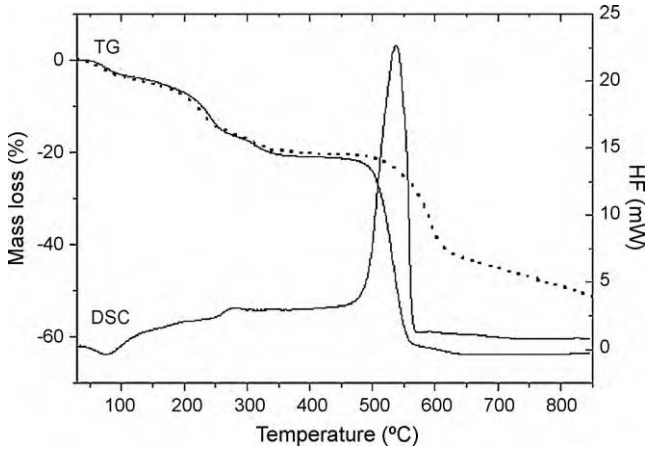

Fig. 3. TG-DSC curves of $[Nd_2pdc_3(dmf)_2]\cdot dmf_{0.5}(H_2O)$ recorded in air (—) and argon (- - -).

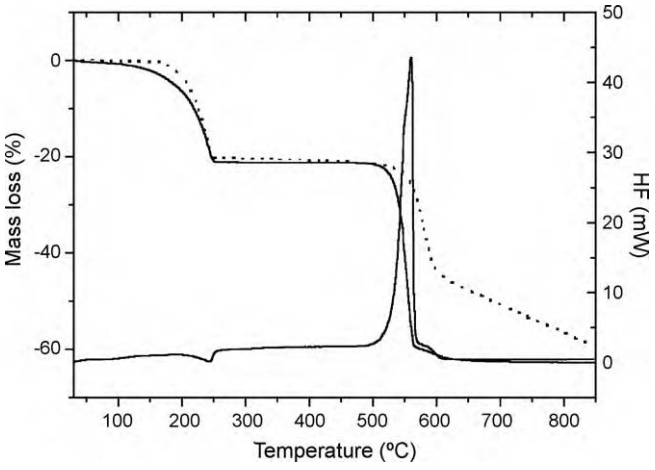

Fig. 4. TG-DSC curves of $[Er_2pdc_3(dmf)_2]\cdot dmf$ recorded in air (—) and argon (- - -).

disordered solvent molecules within the channels. The complexes decompose in two well-separated mass loss stages. The results from thermal decomposition of the investigated compounds in air were given in Table 3. The first weight loss is consistent with departure of uncoordinated as well as covalent bonded solvent molecules whereas the second one is attributed to the decomposition and burning (air) of the desolvated form of complexes.

The as made complexes show a gradual mass loss in a wide temperature range which depending on the nature of the lanthanide ions. An initial mass loss in the range about 30–150 °C is attributed to the removal of weakly bonded water and dmf molecules included in the channels of the frameworks. The release of physically bound solvent molecules is accompanied by a very weak endothermic effect on the DSC curve at about 80 °C. Next, on the TG curve there is observed weight loss due to the removal of N,N′-dimethylformamide molecules coordinated to metal ions (Fig. 3). For the complexes of light lanthanides from La(III) to Sm(III) this process occurs in the two hardly distinguishable steps. The first one takes place in the temperature range about 150–260 °C and is associated with a weak endothermic effect at about 250 °C. The next stage occurs in the temperature range 250–330 °C (except for the cerium complex which is less stable). Among light lanthanide complexes, only lanthanum complex exhibits two very well-separated endothermic effects assigned to the dmf molecules release at 236 °C and 312 °C, respectively. Next, after solvent molecules evolution, slow mass loss is observed due to further decomposition of the unstable network (Table 3).

The proposed way of solvent molecules evolution from the structure of complexes has been confirmed by the TG-FTIR analysis (Fig. 5). The FTIR spectra of gaseous products evolved during heating in the temperature range 30–200 °C show absorption bands only in the wave number 4000–3500 and 1800–1300 cm^{-1} attributed to stretching and deformation vibrations of water molecules [56,57]. These bands are observed during heating of only light lanthanide complexes (from La to Eu). Above this temperature characteristic bands derived from gaseous N,N′-dimethylformamide molecules appear. The bands at 2939 and 2849 cm^{-1} were assigned to the stretching vibrations of the CH bond from the CH_3 groups. The band located at 1724 cm^{-1} can be attributed to the stretching vibrations of the carbonyl CO group. The band at 1493 cm^{-1} was assigned to stretching vibrations of the CN bond. Methyl groups of dmf molecules give characteristic bands derived from asymmetric and symmetric stretching vibrations at 1482 and 1382 cm^{-1}, respectively [63]. Further heating causes collapse of frameworks accompanied by evolution of carbon dioxide molecules giving characteristic doublet bands at 2359, 2343 cm^{-1} and those in the range 750–600 cm^{-1} derived from the valence and deformation vibrations, respectively. At little higher temperature, the FTIR spectra of evolved products show bands at 3075, 3017 and 1217, 1152 cm^{-1} assigned to the stretching and deformation vibrations of C–C and C–N groups from the free pyridine ring [54,57]. At the same time, carbon dioxide and carbon monoxide are released. Carbon monoxide gives an easily detectable double-band with the

Table 3
Thermogravimetric data obtained from TG-DSC curves during heating of $[Ln_2pdc_3(dmf)_2]\cdot(dmf)_x(H_2O)_y$ complexes in air.

Complex	T_1	Removal products	Mass loss (%)		T_2	ΔT_3	Mass loss (%)	
			Calc.	Found			Calc.	Found
$[La_2pdc_3(dmf)_2]\cdot dmf_{0.5}(H_2O)$	30–310	2.5dmf, H_2O	20.59	22.50	–	310–750	66.53	66.30
$[Ce_2pdc_3(dmf)_2]\cdot dmf_{0.5}(H_2O)$	30–250	2.5dmf, H_2O	20.54	20.30	–	250–460	64.99	64.00
$[Pr_2pdc_3(dmf)_2]\cdot dmf_{0.5}(H_2O)$	30–320	2.5dmf, H_2O	24.36	23.70	–	320–570	65.00	65.27
$[Nd_2pdc_3(dmf)_2]\cdot dmf_{0.5}(H_2O)$	30–360	2.5dmf, H_2O	21.27	20.70	–	360–620	64.29	63.54
$[Sm_2pdc_3(dmf)_2]\cdot dmf_{0.5}(H_2O)$	30–330	2.5dmf, H_2O	22.90	22.00	–	330–620	66.25	64.62
$[Eu_2pdc_3(dmf)_2]\cdot dmf_{0.5}(H_2O)$	30–290	2.5dmf, H_2O	20.90	20.30	290–420	420–630	63.23	63.00
$[Gd_2pdc_3(dmf)_2]\cdot dmf_{0.5}(H_2O)$	30–300	2.5dmf, H_2O	19.84	19.00	300–420	420–720	64.12	63.00
$[Tb_2pdc_3(dmf)_2]\cdot dmf$	30–260	3dmf	20.93	22.42	260–460	460–600	63.77	60.50
$[Ho_2pdc_3(dmf)_2]\cdot dmf$	30–260	3dmf	21.07	20.42	260–460	460–600	64.70	64.11
$[Dy_2pdc_3(dmf)_2]\cdot dmf$	30–260	3dmf	20.97	22.00	260–450	450–700	63.81	62.30
$[Er_2pdc_3(dmf)_2]\cdot dmf$	30–250	3dmf	20.89	20.64	250–490	490–700	63.52	62.67
$[Tm_2pdc_3(dmf)_2]\cdot dmf$	30–260	3dmf	20.81	24.18	260–460	460–700	63.40	62.50
$[Yb_2pdc_3(dmf)_2]\cdot dmf$	30–260	3dmf	20.67	21.17	260–480	480–700	62.79	61.36
$[Lu_2pdc_3(dmf)_2]\cdot dmf$	30–260	3dmf	20.58	21.00	260–460	460–700	62.59	61.00

pdc – $C_7H_3NO_4^{2-}$; dmf – C_3H_7NO; T_1 – temperature range of removal solvent molecules from crystal structures of the complexes; T_2 – temperature range of thermal stability of Ln_2pdc_3; T_3 – temperature range of degradation of Ln_2pdc_3 to suitable lanthanide oxides.

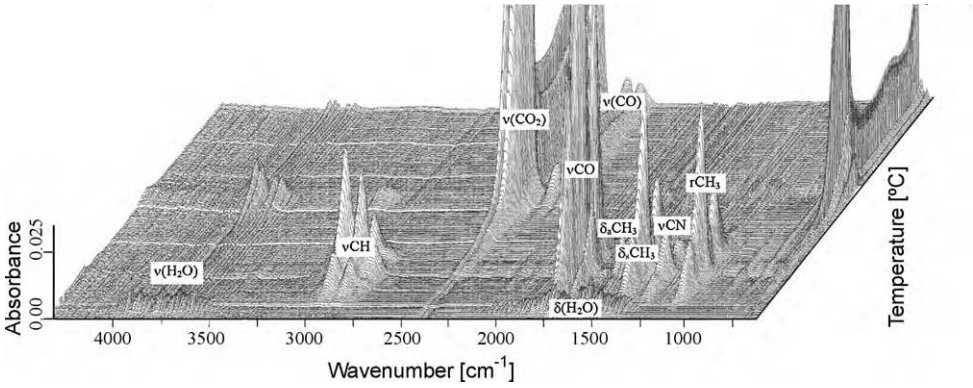

Fig. 5. Stacked plot of FTIR spectra of the evolved gases for $[Nd_2pdc_3(dmf)_2]\cdot dmf_{0.5}(H_2O)$.

maxima at 2177, 2113 cm^{-1}, respectively. Additionally, some bands at 3071, 1605, 1484 and 1448 cm^{-1} are observed. These bands have been assigned to the stretching and deformation vibrations of some hydrocarbons [65]. As the final solid products of thermal decomposition of the complexes in air atmosphere, suitable oxides are formed (Ln_2O_3 for La, Nd, Sm and CeO_2, Pr_6O_{11}).

Thermal decomposition of the complexes from Eu(III) to Lu(III), occurs in a slightly different manner (Fig. 4). During heating in air, similarly to the complexes described earlier, they start to decompose at 30 °C. At first, they lose only physically bonded solvent molecules, included in the channels of the frameworks. Next, on the TG curve, a significant weight loss is observed according to the release of dimethylformamide molecules coordinated with central atoms [34]. This process occurs in one step compared to the light lanthanide complexes and is accompanied by a strong endothermic effect on the DSC curve at about 250 °C. This temperature is diagnostic for the removal of covalently bonded dmf molecules [34]. The values of enthalpy reaction of dmf molecules release are in the range 60–111 kJ/mol. The TG-FTIR spectra of the evolved gaseous products in temperature range 30–260 °C evidently confirm the suggested way of solvent molecules release.

As the product of thermal desolvation, the compounds of the formula $Ln_2(pdc)_3$ are formed. These compounds are stable in a wide temperature range (about 260–460 °C) as can be seen from Table 3. In such temperature range, no weight losses were observed on the TG curve as well as the FTIR spectra do not show any bands that are indicative to formation of stable compounds (Fig. 6). Above 460 °C, further heating results in the decomposition process that is accompanied by evolution of carbon dioxide, carbon monoxide, pyridine and hydrocarbons in the inert atmosphere.

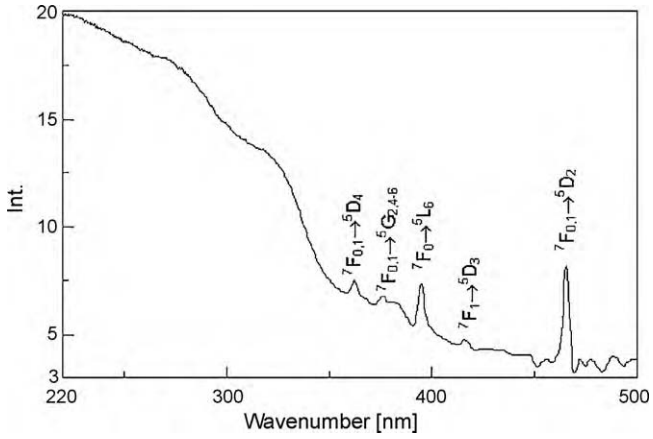

Fig. 7. The excitation spectrum of $[Eu_2pdc_3(dmf)_2]\cdot dmf_{0.5}(H_2O)$ (monitored at 615 nm).

As the final solid products of decomposition of heavier lanthanide dinicotinates in the air atmosphere suitable oxides of the formula Ln_2O_3 (Eu, Gd, Dy, Ho, Er, Tm, Yb, Lu) and Tb_4O_7 are formed.

3.3. Luminescence properties

The $[Eu_2pdc_3(dmf)_2]\cdot dmf_{0.5}(H_2O)$ and $[Tb_2pdc_3(dmf)_2]\cdot dmf$ complexes exhibit strong visible luminescence in the red and green regions, respectively. The excitation spectrum of the europium complex was obtained by monitoring the emission of Eu(III) ions at 615 nm ($^5D_0 \rightarrow {}^7F_2$). As can be seen from Fig. 7, excitation

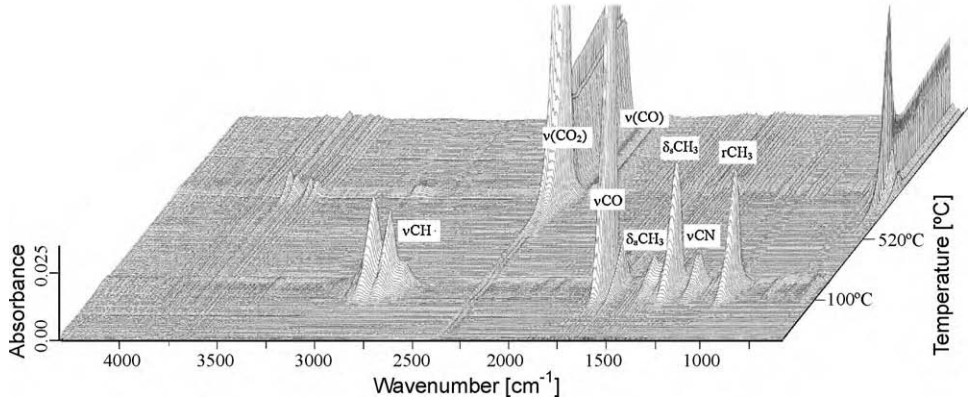

Fig. 6. Stacked plot of FTIR spectra of the evolved gases for $[Er_2pdc_3(dmf)_2]\cdot dmf$.

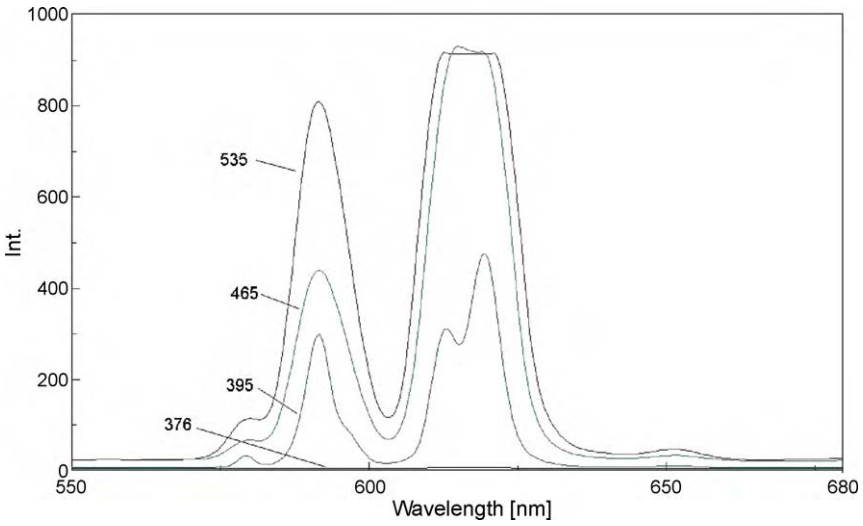

Fig. 8. Comparison of the emission spectra of $[Eu_2pdc_3(dmf)_2]\cdot dmf_{0.5}(H_2O)$ excited at different wavelength (nm).

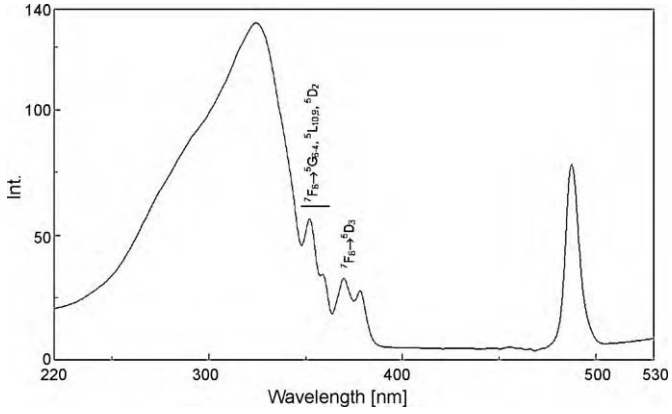

Fig. 9. The excitation spectrum of $[Tb_2pdc_3(dmf)_2]\cdot dmf$ (monitored at 544 nm).

spectrum exhibits a progressive increase of the excitation ability toward shorter wavelengths in the range 220–400 nm which can be assigned to the excited levels of the pdc^{2-} ligands. Additionally, this spectrum shows a series of sharp and relatively weak lines characteristic of the Eu^{3+} energy levels. The lines at 362 nm, 376 nm, 395 nm, 465 nm and 535 nm were assigned to the $^7F_0 \rightarrow {}^5D_4$, $^7F_0 \rightarrow {}^5G_{2,4-6}$, $^7F_0 \rightarrow {}^5L_6$, $^7F_1 \rightarrow {}^5D_3$ and $^7F_0 \rightarrow {}^5D_2$ intrinsic transitions from Eu^{3+}, respectively. These bands were selected as excitation wavelength for the Eu(III) ions as the most intense excitation peaks. The emission spectra of the europium complex, obtained with the different excitation wavelengths are shown in Fig. 8. These spectra consists of several Eu(III) emission peaks due to the $^5D_0 \rightarrow {}^7F_j$ transitions whereas those emission from the ligand are not observed. The bands at 579, 591, 619, 651, and 697 nm were assigned to the $^5{}_0D \rightarrow {}^7F_0$, $^5{}_0D \rightarrow {}^7F_1$, $^5{}_0D \rightarrow {}^7F_2$, $^5{}_0D \rightarrow {}^7F_3$, and $^5{}_0D \rightarrow {}^7F_4$ f-f transitions of Eu(III) ions, respectively. The strongest and most useful emissions for structural determination are observed in the $^5{}_0D \rightarrow {}^7F_1$ and $^5{}_0D \rightarrow {}^7F_2$ transition regions. The $^5{}_0D \rightarrow {}^7F_1$ transition corresponds to a magnetic dipole transition and is relatively unaffected by the local environment. The $^5{}_0D \rightarrow {}^7F_2$ transitions of predominantly electric dipole character are co-called hypersensitive transition because of their sensitivity to the coordination environment [27,29,30]. The transitions at $^5{}_0D \rightarrow {}^7F_3$ and $^5{}_0D \rightarrow {}^7F_4$ are nearly invisible for $[Eu_2pdc_3(dmf)_2]\cdot(dmf)_{0.5}(H_2O)$ complex. As can be seen in Fig. 8, the emission intensities are related to the intrinsic excitation lines

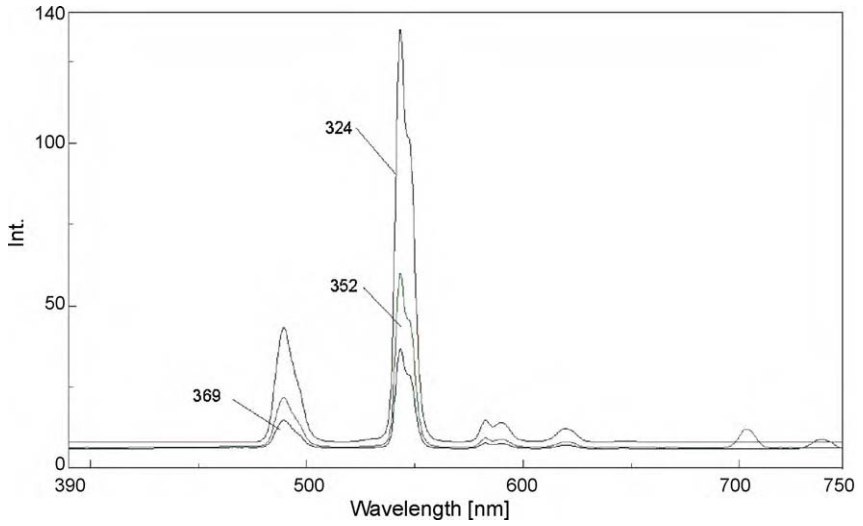

Fig. 10. Comparison of the emission spectra of $[Tb_2pdc_3(dmf)_2]\cdot dmf$ excited at different wavelength (nm).

intensity of europium(III). In this complex, pdc^{2-} ligand shows much weaker intensity than in the $[Tb_2pdc_3(dmf)_2]\cdot dmf$ complex. The stronger emission intensity was obtained rather by the direct an excitation of the lanthanide ions. The similar effect was observed in heterbinuclear complex of Eu(III) and Zn(II) ions [67]. This may be an explanation of such influence of the excitation wavelength on the intensity of emissions.

The excitation spectrum of terbium(III) complex was detected at 544 nm (Fig. 9). The spectrum shows a broad band in the range 220–350 nm with the maximum absorption peak at 324 nm, which can be assigned to the emission of the ligand-to-metal charge transfer processes (LMCT). Additionally, the sharp bands at 352, 369, 378 and 487 nm are observed. The lines at 352 nm, 369 nm and 378 nm were assigned to the $^7F_6 \rightarrow {}^5G_{6-4}$, $^5L_{10,9}$, $^5D_2$ and $^7F_6 \rightarrow {}^5D_3$ transitions, respectively. The intensities of transitions from Tb^{3+} states are relatively weak compared to the emission of the ligand-to-metal charge transfer.

The emission spectrum shown in Fig. 10 under the excitation at 352 nm displays the five emission peaks at 489, 543, 582, 619 and 703 nm, respectively attributed to the intra $4f^8$ $^5D_4 \rightarrow {}^7F_6$, $^5D_4 \rightarrow {}^7F_5$, $^5D_4 \rightarrow {}^7F_4$, $^5D_4 \rightarrow {}^7F_3$ and $^5D_4 \rightarrow {}^7F_2$ transitions of Tb(III) ions. The most intense emission is observed in the region 540–555 nm due to $^5D_4 \rightarrow {}^7F_4$ transition [23,24,34]. The emission bands of the ligand molecules do not appear in the emission spectrum of Tb complex that point to efficient transfer of the excitation energy from ligand to metal. The influence of excitation wavelength on the luminescence intensity also is observed for terbium complex as it can be seen from Fig. 10. When the $[Tb_2pdc_3(dmf)_2]\cdot dmf$ complex was excited with the absorption wavelength of the ligand at 324 nm, the strongest emission of terbium takes place. This excitation energy is absorbed by this ligand and then occurs an efficient energy transfer from ligand triplet state to the europium(III) ions. This excitation process is more efficient that the direct excitation, since the lanthanide cations are characterized by very low absorption coefficient that makes difficult to populate its emitting levels by direct excitation [26,68,69]. These results point to the acting of dinicotinate ligand as “antenna”.

4. Conclusions

Summing up, I have synthesized a series of the isostructural lanthanide complexes with pyridine-3,5-dicarboxylic acid under solvothermal conditions. The polymeric complexes have three-dimensional structures with 1D channels occupied by disordered solvent molecules. The complexes are stable at room temperature but heating causes release of free as and coordinated solvent molecules. The stable intermediate compounds Ln_2pdc_3 are formed during heating complexes of heavier lanthanides (from Eu to Lu). The proposed manner of decomposition has been confirmed by the TG-FTIR spectra of gas-phase products of heating. The complexes $[Eu_2pdc_3(dmf)_2]\cdot dmf_{0.5}(H_2O)$ and $[Tb_2pdc_3(dmf)_2]\cdot dmf$ show very intense luminescence emissions which can be applied in potential chemical sensors design.

References

[1] P.L. Llewellyn, S. Bourrelly, C. Serre, A. Vimont, M. Daturi, L. Hamon, G. de Weireld, J.-S. Chang, D.-Y. Hong, Y.K. Hwang, S.H. Jhung, G. Ferèy, Langmuir 24 (2008) 7245–7250.
[2] S. Bourrelly, P.L. Llewellyn, C. Serre, F. Millange, T. Loiseau, G. Ferèy, J. Am. Chem. Soc. 127 (2005) 13272–13519.
[3] Y. Zou, S. Hong, H. Park, H. Chun, M.S. Lah, Chem. Commun. (2007) 5182–5184.
[4] R. Banerjee, A. Phan, B. Wang, C. Knobler, H. Furukawa, M. O'Keeffe, O.M. Yaghi, Science 319 (2008) 939–943.
[5] H. Hayashi, A.P. Côtè, H. Furukawa, M. O'Keeffe, O.M. Yaghi, Nat. Mater. 6 (2007) 501–506.
[6] B. Chen, C. Liang, J. Yang, O.M. Yaghi, Angew. Chem. Int. Ed. 45 (2006) 1390–1393.
[7] Y. Li, R.T. Yang, Langmuir 23 (2007) 12937–12944.
[8] A. Sudik, A.R. Millward, N.W. Ockwig, A.P. Cote, J. Kim, O.M. Yaghi, J. Am. Chem. Soc. 127 (2005) 7110–7118.
[9] A.G. Wong-Foy, A.J. Matzger, O.M. Yaghi, J. Am. Chem. Soc. 128 (2006) 3494–3495.
[10] T. Loiseau, L. Lecroq, C. Volkringer, J. Marrot, G. Férey, M. Haouas, F. Taulelle, S. Bourrelly, P.L. Llewellyn, M. Latroche, J. Am. Chem. Soc. 128 (2006) 10223–10230.
[11] A.G. Hu, H.L. Ngo, W. Lin, J. Am. Chem. Soc. 125 (2003) 11490–11491.
[12] K.M. Thomas, Catal. Today 120 (2007) 389–398.
[13] M. Dincâ, J.R. Long, J. Am. Chem. Soc. 127 (2005) 9377–9378.
[14] S.S. Kaye, A. Dailly, O.M. Yaghi, J.R. Long, J. Am. Chem. Soc. 129 (2007) 14176–14177.
[15] H. Li, M. Eddaoudi, M. O'Keeffe, O.M. Yaghi, Nature 402 (1999) 276–279.
[16] G. Fèrey, C. Serre, C. Mellot-Draznieks, F. Millange, S. Surblé, J. Dutour, I. Margiolaki, Angew. Chem. Int. Ed. 43 (2004) 6296–6304.
[17] S.S.-Y. Chui, S.M.-F. Lo, J.P.H. Charmant, A.G. Orpen, I.D. Williams, Science 283 (1999) 1148–1150.
[18] K. Uemura, R. Matsuda, S. Kitagawa, J. Solid State Chem. 178 (2005) 2420–2429.
[19] G. Ferey, C. Drazieks-Mellot, Ch. Serre, F. Millange, J. Dutour, S. Surblé, I. Magiolaki, Science 309 (2005) 2040–2042.
[20] S.-Q. Xia, S.-M. Hu, J.-J. Zhang, X.-T. Wu, J.-C. Dai, Z.-Y. Fu, W.-X. Du, Inorg. Chem. Commun. 7 (2004) 271–273.
[21] W.-G. Lu, L. Jiang, X.-L. Feng, T.-B. Lu, Inorg. Chem. 48 (2009) 6997–6999.
[22] H.-S. Wang, B. Zhao, B. Zhai, W. Shi, P. Cheng, D.-Z. Liao, S.P. Yan, Cryst. Growth Des. 7 (9) (2007) 1851–1857.
[23] D.T. de Lill, A. de Bettencourt-Dias, Ch. L. Cahill, Inorg. Chem. 46 (2007) 3960–3965.
[24] P.C.R. Soares-Santos, L. Cunha-Silva, F.A. Almeida-Paz, R.A.Sá. Ferreira, J. Rocha, T. Trindade, L.D. Carlos, H.I.S. Nogueira, Cryst. Growth Des. 8 (7) (2008) 2505–2516.
[25] T. Devic, C. Serre, N. Audebrand, J. Marrot, G. Ferey, J. Am. Chem. Soc. 127 (2005) 12788–12789.
[26] M. Flores, U. Caldiño, G. Córdoba, R. Arroyo, Opt. Mater. 27 (2004) 635–639.
[27] S.V. Eliseeva, J.-C.G. Bŭnzli, Chem. Soc. Rev. 39 (2010) 189–227.
[28] M.D. Allendorf, C.A. Bauer, R.K. Bhakta, R.J.T. Houk, Chem. Soc. Rev. 38 (2009) 1330–1352.
[29] L. Armelao, S. Quici, F. Barigelletti, G. Accorsi, G. Bottaro, M. Cavazzini, E. Tondello, Coord. Chem. Rev. 254 (2010) 487–505.
[30] F.S. Richardson, Chem. Rev. 82 (1982) 541–552.
[31] W.J. Rieter, K.M.L. Taylor, W. Lin, J. Am. Chem. Soc. 129 (2007) 9852–9853.
[32] C. Serre, F. Millange, J. Marrot, G. Férey, Chem. Mater. 14 (5) (2002) 2409–2415.
[33] T.M. Reineke, M. Eddaoudi, M. O'Keeffe, O.M. Yaghi, Angew. Chem. Int. Ed. 38 (17) (1999) 2590–2594.
[34] X. Guo, G. Zhu, F. Sun, Z. Li, X. Zhao, X. Li, H. Wang, S. Qiu, Inorg. Chem. 45 (2006) 2581–2587.
[35] C. Daiguebonne, O. Guillou, K. Boubekeur, Inorg. Chim. Acta 304 (2000) 161–169.
[36] X. Guo, G. Zhu, Z. Li, F. Sun, Z. Yang, S. Qiu, Chem. Commun. (2006) 3172–3174.
[37] K. Liu, H. You, G. Jia, Y. Zheng, Y. Song, M. Yang, Y. Huang, H. Zhang, Cryst. Growth Des. 9 (2009) 3519–3524.
[38] Z.-H. Zhang, T.-H. Okamura, Y. Hasegawa, H. Kawaguchi, L.-Y. Kong, W.-Y. Sun, N. Ueyama, Inorg. Chem. 44 (2005) 6219–6227.
[39] F.A. Almeida Paz, J. Klinowski, Chem. Commun. (2003) 1484–1485.
[40] N.L. Rosi, M. Eddaoudi, J. Kim, M. O'Keeffe, O.M. Yaghi, Angew. Chem. Int. Ed. 41 (2002) 284–287.
[41] X.-J. Zheng, Z.-M. Wang, S. Gao, F.-H. Liao, C.-H. Yan, L.-P. Jin, Eur. J. Inorg. Chem. (2004) 2968–2973.
[42] Q. Shi, S. Zhang, Q. Wang, H. Ma, G. Yang, W.-H. Sun, J. Mol. Struct. 837 (2007) 185–189.
[43] F. Li, Acta Cryst. E63 (2007) m73–m74.
[44] W. Kleist, M. Maciejewski, A. Baiker, Thermochim. Acta 499 (2010) 71–78.
[45] R.L. Fernandes, P.M. Takahashi, R.C.G. Frem, A.V.G. Netto, A.E. Mauro, J.R. Matos, J. Therm. Anal. Calorim. 97 (2009) 153–156.
[46] L.-F. Song, Ch.-H. Jiang, J. Zhang, L.X. Sun, F. Xu, W.-S. You, Y. Zhao, Z.-H. Zhang, M.-H. Wang, Y. Sawada, Z. Cao, J.-L. Zeng, J. Therm. Anal. Calorim. 100 (2010) 679–684.
[47] M. Inoue, H. Kawaji, T. Tojo, T. Atake, Thermochim. Acta 431 (2005) 58–61.
[48] G. Xie, S. Chen, B. Jiao, S. Gao, Q. Shi, Thermochim. Acta 443 (2006) 53–55.
[49] X.-Ch. Lv, Z.-Ch. Tan, Z.-H. Zhang, L.-N. Yang, J.-N. Zhao, L.-X. Sun, T. Zhang, Thermochim. Acta 450 (2006) 102–104.
[50] J. Zhang, J.L. Zeng, Y.Y. Liu, L.X. Sun, F. Xu, W.S. You, Y. Sawada, J. Therm. Anal. Calorim. 91 (1) (2008) 189–193.
[51] V. Logvinenko, D. Dybtsev, V. Fedin, V. Drebushachak, M. Yutkin, J. Therm. Anal. Calorim. 90 (2007) 463–467.
[52] J. Jia, X. Lin, A.J. Blake, N.R. Champness, P. Hubberstey, L. Shao, G. Walker, C. Wilson, M. Schrőder, Inorg. Chem. 45 (2006) 8838–8840.
[53] B. Chen, L. Wang, Y. Xiao, F.R. Fronczek, M. Xue, Y. Cui, G. Qian, Angew. Chem. 121 (2009) 508–511.
[54] R. Łyszczek, J. Therm. Anal. Calorim. 90 (2007) 533–539.
[55] R. Łyszczek, L. Mazur, Z. Rzączyńska, Inorg. Chem. Commun. 11 (2008) 1091–1093.
[56] R. Łyszczek, J. Therm. Anal. Calorim. 93 (2008) 833–838.
[57] R. Łyszczek, J. Anal. Appl. Pyrolysis 86 (2009) 239–244.
[58] Sheldrick, *SHELXS97*, Program for a Crystal Structure Solution, University of Gőttingen, Germany, 1997.

[59] G.M. Sheldrick, *SHELXL97*, Program for the Refinement of a Crystal Structure from Diffraction Data, University of Göttingen, Germany, 1997.
[60] T. Whitfield, L.M. Zheng, X. Wang, A.J. Jacobson, Solid State Sci. 3 (2001) 829–835.
[61] J.Y. Lu, V. Schauss, CrystEngComm 3 (2001) 111–113.
[62] S.-Q. Xia, S.-M. Hu, J.-C. Dai, X.-T. Wu, J.-J. Zhang, Z.-Y. Fu, W.-X. Du, Inorg. Chem. Commun. 7 (2004) 51–53.
[63] G. Durgaprasad, D.N. Sathyanarayana, C.C. Patet, Bull. Chem. Soc. Jpn. 44 (1971) 316–322.
[64] K. McCann, J. Laane, J. Mol. Struct. 890 (2008) 346–358.
[65] S. Holly, P. Sohar, Absorption Spectra in the Infrared Region, Akademiai Kiado, Budapest, 1975.
[66] G.B. Deacon, R.J. Philips, Coord. Chem. Rev. 33 (1980) 227–250.
[67] T.D. Pasatoiu, A.M. Madalan, M.U. Kumke, C. Tiseanu, M. Andruh, Inorg. Chem. 49 (2010) 2310–2315.
[68] L.N. Puntus, K.A. Lyssenko, I.S. Pekareva, J.-C.G. Bünzli, J. Phys. Chem. 113 (2009) 9265–9277.
[69] X. Zhang, J. Lumin. 130 (2010) 1060–1066.